MAGIC upper limits on the high energy emission from GRBs

J. Albert[a], E. Aliu[b], H. Anderhub[c], P. Antoranz[d], A. Armada[b], C. Baixeras[e], J. A. Barrio[d], H. Bartko[f], D. Bastieri[g], J. Becker[h], W. Bednarek[i], K. Berger[a], C. Bigongiari[g], A. Biland[c], R. K. Bock[f,g], P. Bordas[j], V. Bosch-Ramon[j], T. Bretz[a], I. Britvitch[c], M. Camara[d], E. Carmona[f], A. Chilingarian[k], S. Ciprini[l], J. A. Coarasa[f], S. Commichau[c], J. L. Contreras[d], J. Cortina[b], M.T. Costado[m], V. Curtef[h], V. Danielyan[k], F. Dazzi[g], A. De Angelis[n], C. Delgado[m], R. de los Reyes[d], B. De Lotto[n], E. Domingo-Santamaría[b], D. Dorner[a], M. Doro[g], M. Errando[b], M. Fagiolini[o], D. Ferenc[p], E. Fernández[b], R. Firpo[b], J. Flix[b], M. V. Fonseca[d], L. Font[e], M. Fuchs[f], N. Galante[f], R. García-López[m], M. Garczarczyk[f], M. Gaug[g], M. Giller[i], F. Goebel[f], D. Hakobyan[k], M. Hayashida[f], T. Hengstebeck[q], A. Herrero[m], D. Höhne[a], J. Hose[f], C. C. Hsu[f], P. Jacon[i], T. Jogler[f], O. Kalekin[q], R. Kosyra[f], D. Kranich[c], R. Kritzer[a], A. Laille[p], T. Lenisa[n], P. Liebing[f], E. Lindfors[l], S. Lombardi[g], F. Longo[n], J. López[b], M. López[d], E. Lorenz[c,f], P. Majumdar[f], G. Maneva[r], K. Mannheim[a], O. Mansutti[n], M. Mariotti[g], M. Martínez[b], D. Mazin[f], C. Merck[f], M. Meucci[o], M. Meyer[a], J. M. Miranda[d], R. Mirzoyan[f], S. Mizobuchi[f], A. Moralejo[b], K. Nilsson[l], J. Ninkovic[f], E. Oña-Wilhelmi[b], N. Otte[f], I. Oya[d], D. Paneque[f], M. Panniello[m], R. Paoletti[o], J. M. Paredes[j], M. Pasanen[l], D. Pascoli[g], F. Pauss[c], R. Pegna[o], M. Persic[n,s], L. Peruzzo[g], A. Piccioli[o], M. Poller[a], N. Puchades[b], E. Prandini[g], A. Raymers[k], W. Rhode[h], M. Ribó[j], J. Rico[b], M. Rissi[c], A. Robert[e], S. Rügamer[a], A. Saggion[g], A. Sánchez[e], P. Sartori[g], V. Scalzotto[g], V. Scapin[g], R. Schmitt[a], T. Schweizer[f], M. Shayduk[q,f], K. Shinozaki[f], S. N. Shore[t], N. Sidro[b], A. Sillanpää[l], D. Sobczynska[i], A. Stamerra[o], L. S. Stark[c], L. Takalo[l], P. Temnikov[r], D. Tescaro[b], M. Teshima[f], N. Tonello[f], D. F. Torres[b,u], N. Turini[o], H. Vankov[r], V. Vitale[n], R. M. Wagner[f], T. Wibig[i], W. Wittek[f], R. Zanin[b], J. Zapatero[e]

ABSTRACT

The fast repositioning system of the MAGIC Telescope has allowed during its first data cycle, between 2005 and the beginning of year 2006, observing nine different GRBs as possible sources of very high energy gammas. These observations were triggered by alerts from Swift, HETE-II, and Integral; they started as fast as possible after the alerts and lasted for several minutes, with an energy threshold varying between 80 and 200 GeV, depending upon the zenith angle of the burst. No evidence for gamma signals was found, and upper limits for the flux were derived for all events, using the standard analysis chain of MAGIC. For the bursts with measured redshift, the upper limits are compatible

[a]Universität Würzburg, D-97074 Würzburg, Germany

[b]Institut de Física d'Altes Energies, Edifici Cn., E-08193 Bellaterra (Barcelona), Spain

[c]ETH Zurich, CH-8093 Switzerland

[d]Universidad Complutense, E-28040 Madrid, Spain

[e]Universitat Autònoma de Barcelona, E-08193 Bellaterra, Spain

[f]Max-Planck-Institut für Physik, D-80805 München, Germany

[g]Università di Padova and INFN, I-35131 Padova, Italy

[h]Universität Dortmund, D-44227 Dortmund, Germany

[i]University of Łódź, PL-90236 Lodz, Poland

[j]Universitat de Barcelona, E-08028 Barcelona, Spain

[k]Yerevan Physics Institute, AM-375036 Yerevan, Armenia

[l]Tuorla Observatory, Turku University, FI-21500 Piikkiö, Finland

[m]Instituto de Astrofisica de Canarias, E-38200, La Laguna, Tenerife, Spain

[n]Università di Udine, and INFN Trieste, I-33100 Udine, Italy

[o]Università di Siena, and INFN Pisa, I-53100 Siena, Italy

[p]University of California, Davis, CA-95616-8677, USA

[q]Humboldt-Universität zu Berlin, D-12489 Berlin, Germany

[r]Institute for Nuclear Research and Nuclear Energy, BG-1784 Sofia, Bulgaria

[s]INAF/Osservatorio Astronomico and INFN Trieste, I-34131 Trieste, Italy

[t]Università di Pisa, and INFN Pisa, I-56126 Pisa, Italy

[u]ICREA and Institut de Cienciès de l'Espai, IEEC-CSIC, E-08193 Bellaterra, Spain

with a power law extrapolation, when the intrinsic fluxes are evaluated taking into account the attenuation due to the scattering in the Metagalactic Radiation Field (MRF).

Subject headings: gamma rays: bursts — gamma rays: observations

1. Introduction

The physical origin of the enigmatic Gamma-Ray Bursts is still under debate today, 40 years after their discovery (see Mészáros 2006, for a recent review). The possible detection of radiation in the Very High Energy (VHE) region (extending between few tens of GeV and few tens of TeV) will lead to a deeper understanding of the acceleration mechanisms and the emission processes from gamma-ray bursts. The γ-ray emission observed by the Energetic Gamma-Ray Experiment Telescope (EGRET) in some cases extends up to the VHE band (Hurley et al. 1994; Dingus 1995; González et al. 2003), favouring the hypothesis of a highly relativistic source of non-thermal radiation situated in an optically thin region (Piran 1999); more insight, however, can be gained by a clear signal detection in the VHE region, or the evaluation of stringent upper limit in this energy band.

Several observations of GRBs at energies above 100 GeV have been attempted (Götting et al. 2003; Zhou 2003), without showing any indication of a signal. This is due to relatively low sensitivity, as in satellite-borne detectors, or to high energy thresholds, as in the previous generation of Cherenkov telescopes or in particle detector arrays. Only few tentative detections of radiation above 0.1 TeV were reported by MILAGRITO for GRB 970417a (Atkins et al. 2000) and by the GRAND array on GRB 971110 (Poirer et al. 2003).

Upper limits on the prompt or delayed emission of GRBs were also set by Whipple (Connaughton et al. 1997), MILAGRO (Atkins et al. 2005; Saz Parkinson et al. 2005a; Saz Parkinson et al. 2005b; Saz Parkinson et al. 2005c; Saz Parkinson et al. 2006a; Saz Parkinson et al. 2
STACEE (Jarvis et al. 2005) and HEGRA-Airobicc (Padilla et al. 1998).

Imaging Atmospheric Cherenkov Telescopes (IACT) of the latest generation achieve a better flux sensitivity and a lower energy threshold, and thus are better suited to detect VHE γ-rays; on the other hand, their small fields of view permit unguided observations only by virtue of serendipitous detection, and they have to rely on an external trigger, such as that provided by automated satellite link to the GRB Coordinates Network (GCN), which broadcasts the coordinates of events triggered and selected by dedicated satellite detectors.

Among the new Cherenkov telescopes, MAGIC (Mirzoyan 2005) is best suited for the

detection of the prompt emission of GRBs, because of its low energy threshold, large effective area and, in particular, its capability for fast slewing (Bretz et al. 2003). The low trigger threshold, currently 50 GeV at zenith, should allow the observation of GRBs even at large redshift, as lower energy radiation can effectively reach Earth without interacting much with the MRF. Moreover, in its fast-slewing mode, MAGIC can be repositioned within 30 s to any position on the sky; in case of a target-of-opportunity alert by GCN, an automated procedure takes only few seconds to terminate any pending observation, validate the incoming signal, and start slewing toward the GRB position. Up to now, the current maximal repositioning time is ~ 100 s. In two cases, this allowed to put upper limits on the GRB flux even during the prompt emission (Galante et al. 2005; Albert et al. 2006; Morris et al. 2006b).

The detection of VHE radiation from the GRB is important for comparing different theoretical models. The emission in the GeV-TeV range in the prompt and delayed phase is predicted by several authors (see Zhang & Mészáros 2001; Pe'er & Waxman 2004; Razzaque et al. 2004, for a detailed analysis). Possible processes comprise leptonic and hadronic models: inverse-Compton (IC) scattering by electrons in internal (Papathanassoiu & Mészáros 200 Pilla & Loeb 1998) or external shocks (Mészáros et al. 1994), IC in the afterglow shocks (Dermer et al. 2000; Zhang & Mészáros 2001; Derishev et al. 2001; Wang et al. 2001), IC by electrons responsible for optical flashes (Beloborodov 2005), and pure electron-synchrotron (Zhang & Mészáros 2001); proton-synchrotron emission (Totani 2000), photon-pion production (Waxman 1995; Böttcher & Dermer 1998; Chiang & Dermer 1999; Li et al. 2002; Fragile et al. 2004), and neutron cascades (Bahcall & Mészáros 2000; Derishev et al. 1999; Rossi et al. 2006).

During the early afterglow phase, the recent observations by the Swift satellite of X-ray flares lasting $10^3 \div 10^4$ s (Burrows et al. 2005) suggested the possibility of correlated γ-ray emission extending into the GeV-TeV region, where the strong VHE flares are predicted to originate from IC scattered photons in the forward shock (Wang et al. 2006).

Measurements in this energy range can be used to test all these competing models. However, as most of the observed GRBs occur at large redshift, strong attenuation of the VHE γ-ray flux is expected, as a result of the interaction with low energy photons of the Metagalactic Radiation Field (Nikishov 1961; de Jager & Stecker 2002). The knowledge of the redshift, therefore, is important for a precise interpretation (Mannheim et al. 1996).

In this article, we report on the analysis of data collected on several GRBs followed by MAGIC during their prompt emission and early afterglow phases.

2. Gamma-ray analysis with the MAGIC telescope

The Major Atmospheric Gamma Imaging Cherenkov (MAGIC) telescope (Mirzoyan 2005), located on the Canary Island of La Palma (2200 m asl, 28°45′ N, 17°54′ W), completed its commissioning phase in early fall 2004. MAGIC is currently the largest IACT, with a 17 m diameter tessellated reflector dish consisting of 964 0.5×0.5 m^2 diamond-milled aluminium mirrors. In its current configuration, the MAGIC photo-multiplier camera has a trigger region of 2.0° diameter (Cortina et al. 2005), and a trigger collection area for γ-rays of the order of 10^5 m^2, which increases further with the zenith angle of observation. Presently, the accessible trigger energy range spans from 50-60 GeV (at small zenith angles) to tens of TeV. The MAGIC telescope is focused to 10 km distance – the most likely position for a 50 GeV γ-shower. The accuracy in reconstructing the direction of incoming γ-rays, the point spread function (PSF), is about 0.1°, slightly depending on the analysis.

The reconstructed signals are calibrated (Gaug et al. 2005), and then cleaned of spurious backgrounds from the light of the night sky using two different image cleaning procedures: one algorithm requiring signal exceeding fixed reference levels, and a second algorithm employing additionally the reconstruced arrival time information (Gaug 2006). Non-physical background images are eliminated (e.g. car flashes having triggered the readout). Events are processed by means of the MAGIC standard analysis software (Bretz et al. 2005), using the standard Hillas analysis (Hillas 1985; Fegan et al. 1997). Gamma/hadron separation is performed by means of the Random Forest (RF) method (Breiman 2001), a classification method that combines several parameters describing the shape of the image into a new parameter called *hadronness* (Hengstebeck 2006), the final γ/hadron discriminator in our analysis. Monte Carlo samples are used to optimize, as a function of energy, the cuts in hadronness. The energy of the γ-ray is also estimated using a RF approach, yielding a resolution of $\sim 30\%$ at 200 GeV. The parameter *alpha* of the Hillas analysis, which is related to the direction of the incoming shower, is not included in the calculation of hadronness; it is used separately to evaluate the significance of a signal. If the telescope is directed at a point-like γ-ray source, as a GRB is expected to be, the alpha-distribution of collected photons should peak at 0°, while it is uniform for isotropic background showers.

3. Blind Test with Crab Nebula

On 2005 October 11 at 02:17:37 UT, the Integral satellite announced GRB 051011[1] at the position J2000 R.A. = $5^{\rm h}\,34^{\rm m}\,47^{\rm s}$, decl. = $+21^\circ\,54'\,39''$. A few hours later, Integral sent a new GCN (Mereghetti & Mowlavi 2005) stating that GRB 051011 was in fact the Crab Nebula. Thus, in a blind test, we acquired 2814 seconds of events coming from the Crab Nebula, the standard source of γ-rays at VHE energies. The analysis yielded a 14σ signal above 350 GeV (Scapin et al. 2006), showing that MAGIC can observe, at 5σ level, spectra of 5 Crab Units (1 C.U. = 6.57×10^{-10} cm^{-2} s^{-1} above 100 GeV) of intensity in 40 s, if above 300 GeV, and in 90 s if below 300 GeV.

4. GRBs observed by MAGIC during its first observation cycle

An automatic alert system has been operational from 2004 July 15. Since then, about 200 GRBs were detected by HETE-II, Integral and Swift, out of which about 100 contained GRB coordinates. Time delays to the onset of the burst were of the order of several seconds to tens of minutes. During the first MAGIC data cycle, between April 2005 and March 2006, 9 GRBs were observed by MAGIC during the prompt or the early afterglow emission phase, as listed in Table 1.

4.1. GRB 050421

GRB 050421 was detected by the Burst Alert Telescope (BAT) on board Swift at 04:11:52 UT. The BAT light curve and flux are shown in figure 1. Coordinates were R.A. = $20^{\rm h}\,28^{\rm m}\,58^{\rm s}$, decl. = $+73^\circ\,39'\,54''$ with an uncertainty of 4 arcmin (Barbier et al. 2005a). Its duration in the 15-350 keV range is 10.3 s with a total fluence of 1.8×10^{-7} erg cm^{-2}. The other telescope on board Swift, the X-Ray Telescope (XRT), could observe the burst in the 0.2-10 keV range since $T_0 + 116$ s until $T_0 + 591$ s whose light curve can be described by a broken power law, i.e. the achromatic break has been observed at $T_0 + 147$ s. Figure 1 shows the X-ray light curve of this burst. No optical counterpart was observed, thus GRB 050421 has been catalogued as a dark burst.

[1]IBAS alert nr. 2673, see at `http://ibas.mi.iasf.cnr.it/`

	Burst	Satellite	T_0 [UT]	$\Delta T_{\rm alert}$	$\Delta T_{\rm start}$	$t_{\rm slewing}$	zenith angle
1.	GRB 050421	Swift	04:11:52	58 s	108 s	26 s	$\sim 52°$
2.	GRB 050502a	Integral	02:13:57	39 s	689 s	223 s	$\sim 30°$
3.	GRB 050505	Swift	23:22:21	540 s	717 s	90 s	$\sim 49°$
4.	GRB 050509a	Swift	01:46:29	16 s	131 s	108 s	$\sim 58°$
5.	GRB 050713a	Swift	04:29:02	13 s	40 s	17 s	$\sim 49°$
6.	GRB 050904	Swift	01:51:44	82 s	145 s	54 s	$\sim 24°$
7.	GRB 060121	HETE-II	22:24:54	15 s	583 s	–	$\sim 48°$
8.	GRB 060203	Swift	23:55:35	171 s	268 s	84 s	$\sim 44°$
9.	GRB 060206	Swift	04:46:53	16 s	59 s	35 s	$\sim 13°$

Table 1: Summary of GRBs observed by MAGIC from April 2005 to March 2006. $\Delta T_{\rm alert}$ stands here for the time delay after T_0 until the burst coordinates were received from the GCN. $\Delta T_{\rm start}$ is the total time delay before the observation could be started, of which $t_{\rm slewing}$ is the time lost for repositioning the telescope.

4.2. GRB 050502a

GRB 050502a was triggered by Integral at 02:13:57 UT. The light curve is shown on the left hand side of figure 2. Coordinates were R.A. = $13^{\rm h}\,29^{\rm m}\,46^{\rm s}$, decl. = $42°\,40'\,27''$ with an uncertainty of 2 arcmin (Gotz 2005a). Its duration is 20 s in the 20-200 keV range with a total fluence of 1.4×10^{-6} erg cm^{-2} and a peak flux of 1×10^{-7} erg cm^{-2} s^{-1} (Gotz 2005b). No X-ray counterpart was observed, but an optical afterglow followed the burst (Gotz 2005a; Durig 2005), a tentative redshift measurement gives $z = 3.793$.

4.3. GRB 050505

GRB 050505 was triggered by BAT at 23:22:21 UT. Coordinates were R.A. = $9^{\rm h}\,27^{\rm m}\,03^{\rm s}$, decl. = $+30°\,16'\,21''$ with an uncertainty of 4 arcmin (Hurkett et al. 2005a). It was a long burst with $T_{90} = 60$ s in the 15-350 keV range and a total fluence of 4.1×10^{-6} erg cm^{-2} (Hullinger et al. 2005). There are three further short spikes at T_0+23.3 s, T_0+30.4 s and T_0+50.4s, as shown in figure 3. Both X-ray and optical observations followed the burst, providing a redshift measurement of $z = 4.27$.

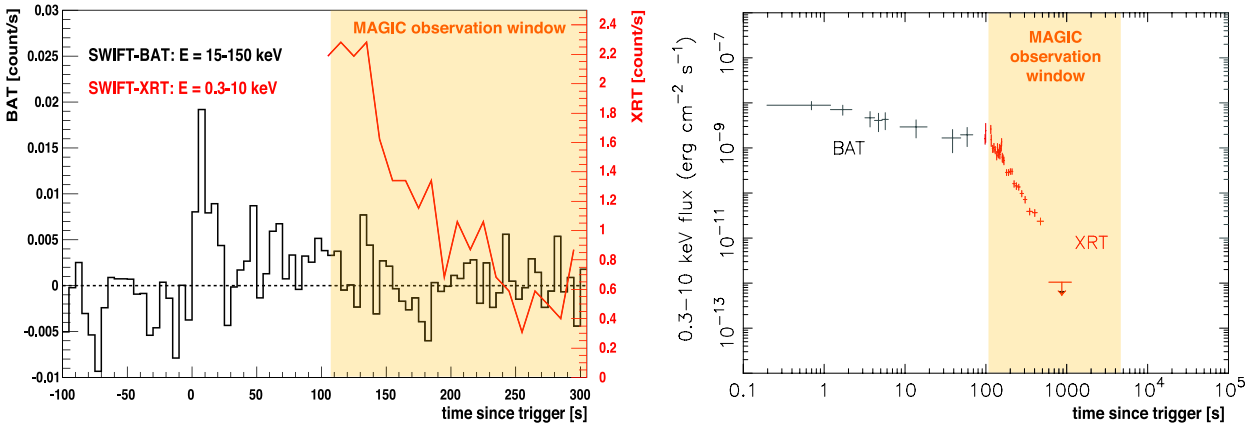

Fig. 1.— Left: Light curve of GRB 050421 in two energy ranges measured by BAT and XRT. Because of low event rate, time bins of 5 s for the BAT and 10 s for XRT were selected. Right: Flux of GRB 050421 measured by BAT and XRT. The orange shadowed area represents the MAGIC observation time window and the overlap with Swift data.

4.4. GRB 050509a

GRB 050509a was triggered by BAT at 01:46:28 UT. The BAT light curve is shown in figure 4. Coordinates were R.A. = $20^{\rm h}\,42^{\rm m}\,20^{\rm s}$, decl. = $+54^\circ\,04'\,16''$ with an uncertainty of 3 arcmin (Hurkett et al. 2005b). Its duration was $T_{90} = 13$ s in the 15-350 keV range with a total fluence of 4.6×10^{-7} erg cm^{-2} (Barbier et al. 2005b). Only an X-ray counterpart could be observed at later times by the XRT instrument and no redshift measurement was possible.

4.5. GRB 050713a

This burst is of particular interest being the first burst observed by MAGIC during its prompt emission (Albert et al. 2006). On 13$^{\rm th}$ July 2005 at 04:29:02 UT the BAT instrument detected a burst located at R.A. = $21^{\rm h}\,22^{\rm m}\,09^{\rm s}.53$, decl. = $+77^\circ\,04'\,29''.50 \pm 3'$ (Falcone et al. 2005). The MAGIC alert system received and validated the alert 13 s after the burst, data taking started 40 s after the burst original time T_0 (Galante et al. 2005).

The burst was classified as a bright burst by Swift with a duration of $T_{90} = 70 \pm 10$ s. The brightest part of the keV emission occured within $T_0 + 20$ s, three smaller peaks followed at $T_0 + 50$ s, $T_0 + 65$ s and $T_0 + 105$ s, while a *pre-burst* peak took place at $T_0 - 60$ s (see figure 5). The spectrum, over the interval from $T_0 - 70$ s to $T_0 + 121$ s, can be fitted with a

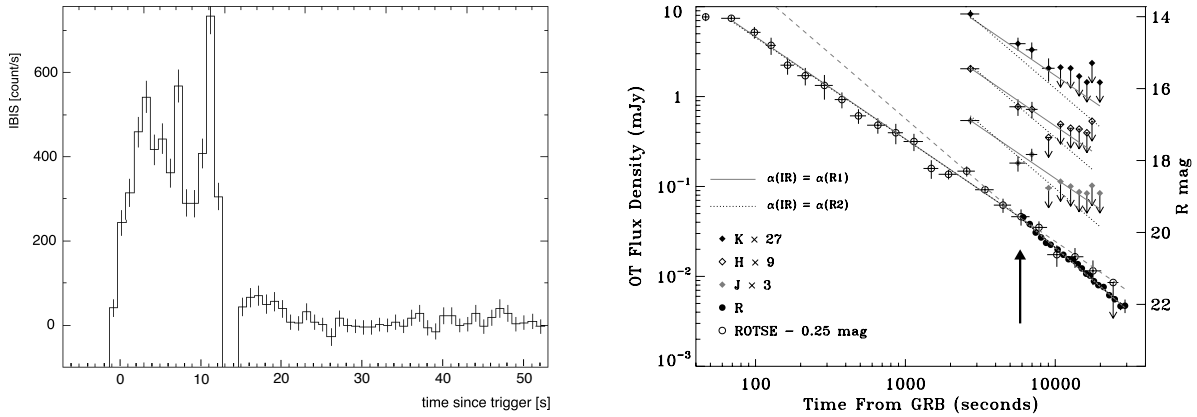

Fig. 2.— Left: Light curve of GRB 050502a measured by Integral (figure from http://ibas.mi.iasf.cnr.it/IBAS_Results.html). Right: Light curves of the optical and IR data of GRB 050502a. The optical light curve is fitted to a broken power law t^{α}, steepening from $\alpha = -1.13 \pm 0.02$ to -1.44 ± 0.02 at ~ 5700 s. The arrow denotes the break time. Figure from (Yost et al. 2006).

power law with photon index -1.58 ± 0.07 and yields a fluence of 9.1×10^{-6} erg cm^{-2} in the 15-350 keV range (Palmer et al. 2005). The burst triggered also the Konus-Wind satellite (Golenetskii et al. 2005), which measured the spectrum of the burst during the first 16 s, that is the duration of the first big peak as reported by Swift. In the local coordinate system of MAGIC, GRB 050713a was located at an azimuth angle of $-6°$ (near North) and a zenith angle of 50°. The sky region of the burst was observed during 37 min, until twilight.

4.6. GRB 050904

Also this burst is of particular interest, being the second and the latest burst with prompt emission observed by MAGIC. It was triggered at 01:51:44 UT by BAT, coordinates were R.A. $= 0^{\rm h}\,54^{\rm m}\,50^{\rm s}.79$, decl. $= +14°\,05'\,09''.42 \pm 3'$ (Cummings et al. 2005). XRT slewed promptly and started the observation at $T_0 + 161$ s, revealing an uncatalogued fading source. It is a long burst ($T_{90} = 225$ s) with a total fluence of 5.4×10^{-6} erg cm^{-2} in the 15-150 keV range (Sakamoto et al. 2005). This burst is the most distant burst ever observed, with an estimated redshift $z = 6.29$ (Kawai et al. 2005). Its X-ray light curve (see figure 6) shows the recently discovered flares, temporary re-brightening of the X-ray emission at later times.

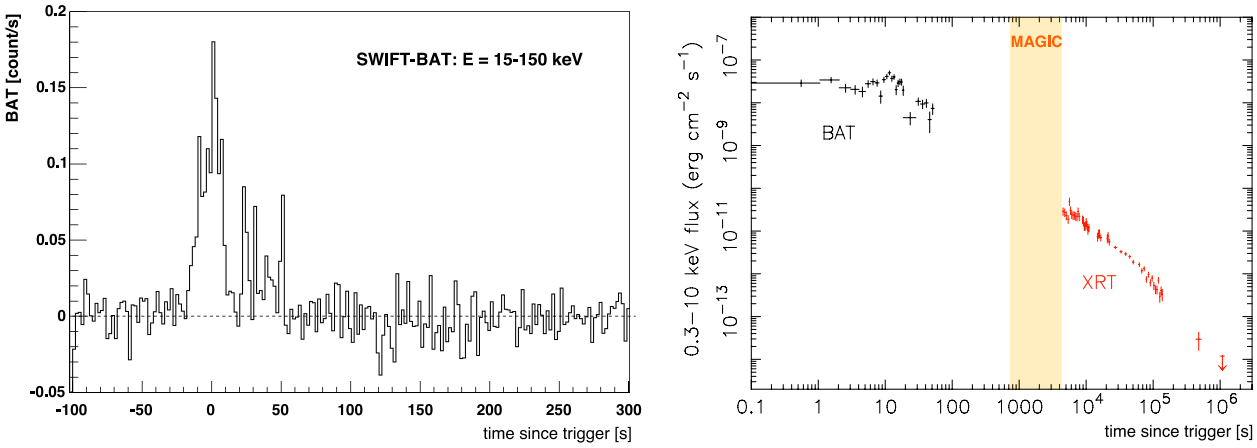

Fig. 3.— Left: Light curve of GRB 050505 measured by BAT. There is no overlap between the BAT and XRT observations. The time bins of the light curve are 2 s. Right: Flux of GRB 050505 measured by BAT and XRT. The orange shadowed area represents the MAGIC observation time window, starting 717 s after the burst onset.

4.7. GRB 060121

HETE II triggered this short and hard Gamma-Ray Burst at 22:24:54 UT, with coordinates R.A. = $09^{\rm h}\ 09^{\rm m}\ 52^{\rm s}.18$, decl. = $+45^\circ\ 39'\ 37''.42 \pm 3'$ with a $T_{90} = 2$ s in the 20 keV - 1 MeV energy range (Arimoto et al. 2006; Golenetskii et al. 2006). Its X-ray light curve is shown in figure 7. In the same energy range the total fluence is estimated to 4.7×10^{-6} erg cm^{-2}, with a peak flux of 1.64×10^{-5} erg cm^{-2} s^{-1}. Also XRT observed the afterglow and detected a fading X-ray source inside the HETE II error box (Mangano et al. 2006). An optical counterpart was not confirmed by TNG, which did, however, detect a weak source inside the XRT error box (Malesani et al. 2006). Moreover, HST gave no evidence of an optical afterglow, although the burst lies close to a faint red galaxy at high redshift (Levan et al. 2006).

4.8. GRB 060203

Triggered by BAT at 23:55:35 UT with coordinates R.A. = $06^{\rm h}\ 54^{\rm m}\ 03^{\rm s}.85$, decl. = $+71^\circ\ 48'\ 38'' \pm 40''$ (Barthelmy et al. 2006). The BAT light curve is shown in figure 8. It is a long burst with $T_{90} = 60$ s and fluence of 8.5×10^{-7} erg cm^{-2} in the 15-150 keV energy range.

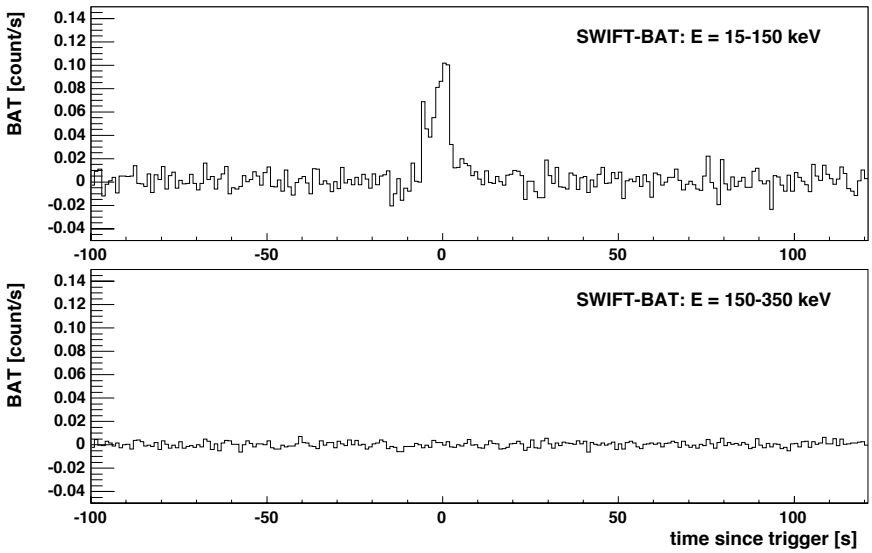

Fig. 4.— Light curve of GRB 050509a in two energy bins measured by BAT. The lower plot illustrates - representatively for all BAT data - that the BAT mask is transparent for energies above 150 keV and no emission can be measured at higher energies. The time resolution is 1 s per bin.

4.9. GRB 060206

This last burst was also triggered by BAT at 04:46:53 UT with coordinates R.A. = $13^{\rm h}\ 31^{\rm m}\ 43^{\rm s}.42$, decl. = $+35^\circ\ 03'\ 03''.60 \pm 3'$ (Morris et al. 2006a). The BAT light curve shows a single gaussian peak structure from $T_0 - 1$ to $T_0 + 10$ s (see figure 9), for a total $T_{90} = 11$ s and a fluence in the 15-350 keV of 8.4×10^{-7} erg cm^{-2} (Palmer et al. 2006). No clear measurement of the jet-break was possible. A redshift measurement gives a value of $z = 4.05$ (Aoki et al. 2006), which makes it a very distant source and strong absorption effects are expected.

5. Results

All nine GRBs were analyzed using the MAGIC standard analysis described above. In this work the image cleaning algorithm using also arrival time information was used, as showing more robust results at low energies. For each GRB a dedicated OFF-source data set was selected on the basis of being compatible with the ON-data with respect to several parameters: zenith angle, as the effective area depends strongly on it; local brightness of the sky, depending mostly on Moon phase and zenith angle; trigger rate, depending

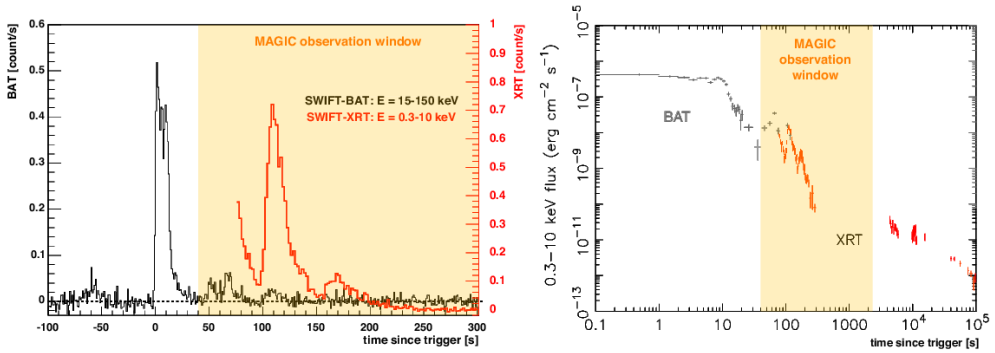

Fig. 5.— Left: Light curve of GRB 050713a measured by BAT and XRT in two different energy ranges. The time binning is 1 s for BAT and 2 s for XRT. Right: Flux of the prompt and afterglow emission measured by BAT and XRT. The orange shadowed area illustrates the observation time window of MAGIC.

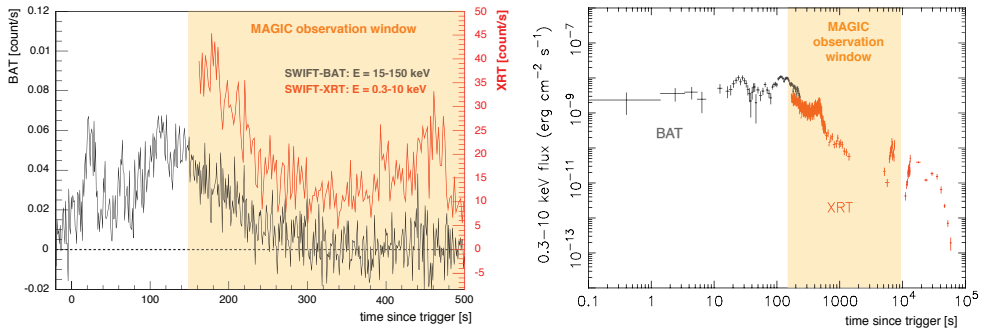

Fig. 6.— Left: Light curve of GRB 050904 in two energy ranges measured by BAT and XRT. The time resolution is 1 s per bin. Right: Flux measured by BAT and XRT in the prompt and afterglow emission. The MAGIC observation window is shown shadowed.

mostly on atmospheric transparency and on hardware settings. Loose preliminary cuts were used to remove unphysical events. After training of the RF, for each burst a *hadronness* cut was applied which could grant about 90% efficiency on γ-ray events according to the corresponding Monte Carlo, in order to keep high statistics of possible γ-rays events.

The analysis showed no evident signal excess, as can be seen in figure 10. For each burst the *alpha* plot over the whole data set and for reconstructed energies greater than 100 GeV is shown. The *alpha* distributions of the GRB data sets are flat, as expected from background hadronic events, and are compatible with the corresponding OFF-source data set. No excess in the signal region, i.e. for $alpha < 30°$, can be seen.

No excess was also evidenced using a temporal analysis: The entire data taking interval

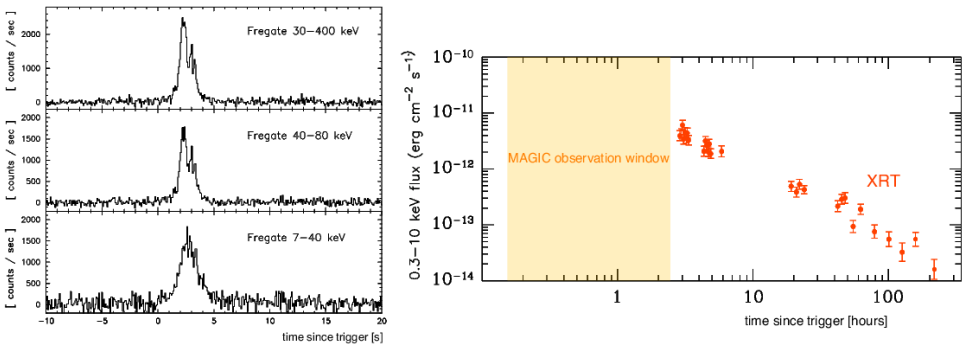

Fig. 7.— Left: Light curve of GRB 060121 measured by HETE Fregate in three different energy bins. Figure from (Donaghy et al. 2006). Right: Flux of the afterglow measured by Swift XRT detector. MAGIC observation window is shown as orange area.

was divided into 20-second time bins and the number of potential γ-ray events, extracted from the alpha distribution; they are shown in the light curves of Figure 11: red filled circles denote the excess events, blue open circles the background events (offset by 5 from excess counts in order to make the plot more readable). The distributions of excess events remain zero on average during the observation, and no significant variation of the sample average is visible with time.

Upper limits have been derived for the first 30 minutes of each burst using the Rolke approach (Rolke et al. 2005). A systematic uncertainty of 30% on the efficiency has been considered in the upper limit calculation. Table 2 summarizes the upper limits derived for all nine GRBs during the first 30 minutes of data taking.

6. Discussion

A preliminary estimate of the observability of GRBs by the MAGIC telescope had originally been derived using the fourth BATSE catalogue (Bastieri et al. 2005; Galante 2006). The GRB spectra were extended to GeV energies with a simple power law and using the observed high-energy spectral index. The extrapolated fluxes were finally compared to the estimated MAGIC sensitivity. Setting conservative cuts on observation times and significances, and assuming an energy threshold of 30 GeV, a $5\,\sigma$-signal rate of $0.5-2$ per year was obtained for an assumed observation delay between 15 and 60 s and a BATSE trigger rate of $\sim$360/year. Taking into account the rate of GRBs (Guetta et al. 2003), and extrapolating GRB spectra, as observed by BATSE, to VHE using an unbroken power law of reasonable power index (Preece et al. 2000), it was foreseen that MAGIC could detect about one GRB

	Energy	Fluence Upper Limit		
	[GeV]	[cm^{-2} keV^{-1}]	[erg cm^{-2}]	C.U.
GRB 050421	212.5	5.26×10^{-16}	3.80×10^{-8}	0.20
	275.8	3.64×10^{-16}	4.43×10^{-8}	0.27
	366.4	5.21×10^{-17}	1.12×10^{-8}	0.08
	658.7	2.07×10^{-17}	1.41×10^{-8}	0.14
GRB 050502	152.3	1.67×10^{-15}	6.21×10^{-8}	0.27
	219.3	2.83×10^{-15}	2.18×10^{-7}	1.15
	275.8	1.13×10^{-15}	1.37×10^{-7}	0.83
	360.8	7.57×10^{-17}	1.58×10^{-8}	0.11
	629.1	5.62×10^{-17}	3.56×10^{-8}	0.35
GRB 050505	212.9	2.03×10^{-15}	1.48×10^{-7}	0.76
	275.1	2.66×10^{-15}	3.22×10^{-7}	1.94
	363.6	5.28×10^{-16}	1.11×10^{-7}	0.79
	704.1	1.85×10^{-17}	1.46×10^{-8}	0.15
GRB 050509a	215.1	1.04×10^{-15}	7.69×10^{-8}	0.40
	273.4	1.39×10^{-15}	1.67×10^{-7}	1.00
	362.8	7.74×10^{-16}	1.63×10^{-7}	1.15
	668.5	1.69×10^{-16}	1.21×10^{-7}	1.22
GRB 050713a	169.9	3.63×10^{-15}	1.68×10^{-7}	0.76
	212.5	1.12×10^{-15}	8.08×10^{-8}	0.42
	275.8	2.07×10^{-15}	2.52×10^{-7}	1.52
	366.4	3.33×10^{-16}	7.16×10^{-8}	0.51
	658.7	2.24×10^{-17}	1.55×10^{-8}	0.15
GRB 050904	85.5	9.06×10^{-15}	1.06×10^{-7}	0.32
	140.1	3.00×10^{-15}	9.42×10^{-8}	0.38
	209.9	2.18×10^{-15}	1.53×10^{-7}	0.79
	268.9	5.82×10^{-16}	6.74×10^{-8}	0.40
	355.2	5.01×10^{-16}	1.11×10^{-7}	0.71
	614.9	1.26×10^{-16}	7.63×10^{-8}	0.73

	Energy	**Fluence Upper Limit**		
	[GeV]	**[cm^{-2} keV^{-1}]**	**[erg cm^{-2}]**	**C.U.**
GRB 060121	151.3	2.64×10^{-15}	9.67×10^{-8}	0.41
	212.8	6.57×10^{-16}	4.76×10^{-8}	0.25
	273.7	2.13×10^{-16}	2.56×10^{-8}	0.15
	367.7	4.47×10^{-16}	9.66×10^{-8}	0.69
	636.4	4.84×10^{-17}	3.14×10^{-8}	0.31
GRB 060203	151.5	1.10×10^{-14}	4.03×10^{-7}	1.71
	219.5	5.07×10^{-16}	3.91×10^{-8}	0.21
	274.0	1.57×10^{-16}	1.88×10^{-8}	0.11
	365.3	3.54×10^{-16}	7.56×10^{-8}	0.54
	639.5	4.45×10^{-17}	2.91×10^{-8}	0.29
GRB 060206	85.5	1.23×10^{-14}	1.44×10^{-7}	0.44
	139.9	9.83×10^{-16}	3.08×10^{-8}	0.13
	210.3	5.50×10^{-16}	3.89×10^{-8}	0.20
	269.2	3.65×10^{-16}	4.23×10^{-8}	0.25
	355.4	6.47×10^{-16}	1.31×10^{-7}	0.91
	614.0	2.88×10^{-17}	1.74×10^{-8}	0.17

Table 2: Derived fluence upper limits for the first 30 minutes of data of nine Gamma-Ray Bursts.

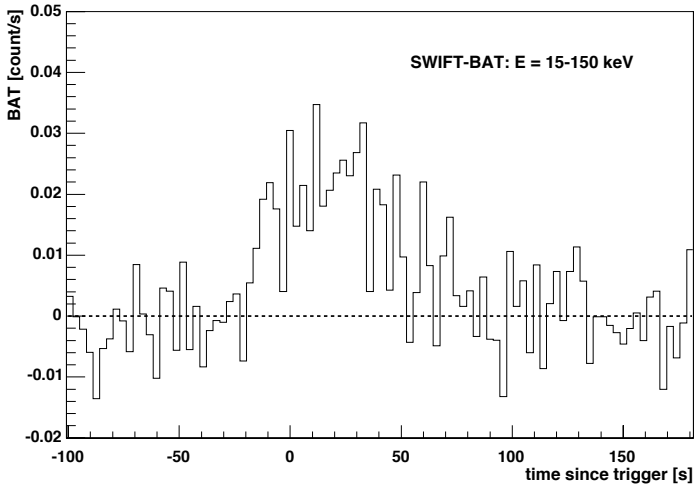

Fig. 8.— Light curve of GRB 060203 measured by BAT. The time resolution is 3 s per bin.

per year at a 5σ level. A maximal redshift up to $z = 2$ was considered.

This estimate must be revised: the Swift alert rate is about a factor 2 lower than predicted, and it includes bursts even fainter than those observed by BATSE; also, for these bursts the effective MAGIC energy threshold at analysis level was higher than the assumed one ($\sim$ 80 GeV); most important, the distribution of bursts detected by Swift has a much higher median redshift than expected. As a result, the number of GRBs that MAGIC can detect is now estimated to lie in the range of 0.2-0.7 per year. This number can be expected to increase again with the launch of the GLAST satellite, and the increased number of alerts due to the GRB monitoring by both GLAST and Swift.

7. Conclusions

MAGIC was able to observe part of the prompt and the early afterglow emission phase of many GRBs as a response to the alert system provided by several satellites. No excess events above $\sim$ 100 GeV were detected, neither during the prompt emission phase nor during the early afterglow. We have derived upper limits for the γ-ray flux between 85 and 1000 GeV. These limits are compatible with a naive extension of the power law spectrum, when the redshift is known, up to hundreds of GeV.

For the first time a Cherenkov telescope has been shown able to perform direct rapid observations of the prompt emission phase of GRBs. This is particulary relevant in the so called "Swift era". Although strong absorption of the high-energy γ-ray flux by the

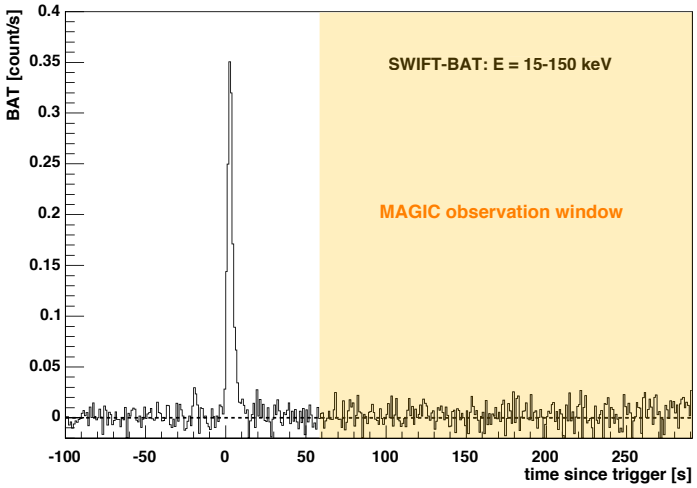

Fig. 9.— Light curve of GRB 060206 measured by BAT, sampled in bins of 1 s. The beginning of MAGIC observation is shown shadowed.

MRF is expected at high redshifts, given its sensitivity to low fluxes and its fast slewing capabilities, the MAGIC telescope is currently expected to detect about 0.5 GRBs per year, if the GRB spectra extend to the energy domain of hundreds of GeV, following a power law with reasonable indices.

Acknowledgments

The construction of the MAGIC Telescope was mainly made possible by the support of the German BMBF and MPG, the Italian INFN, and the Spanish CICYT, to whom goes our grateful acknowledgement. We would also like to thank the IAC for the excellent working conditions at the Observatorio del Roque de los Muchachos in La Palma. This work was further supported by ETH Research Grant TH 34/04 3 and the Polish MNiI Grant 1P03D01028.

Facilities: MAGIC

REFERENCES

Albert, J., et al. 2006, ApJ, 641, L9

Aoki, K., et al. 2006, GCN 4703

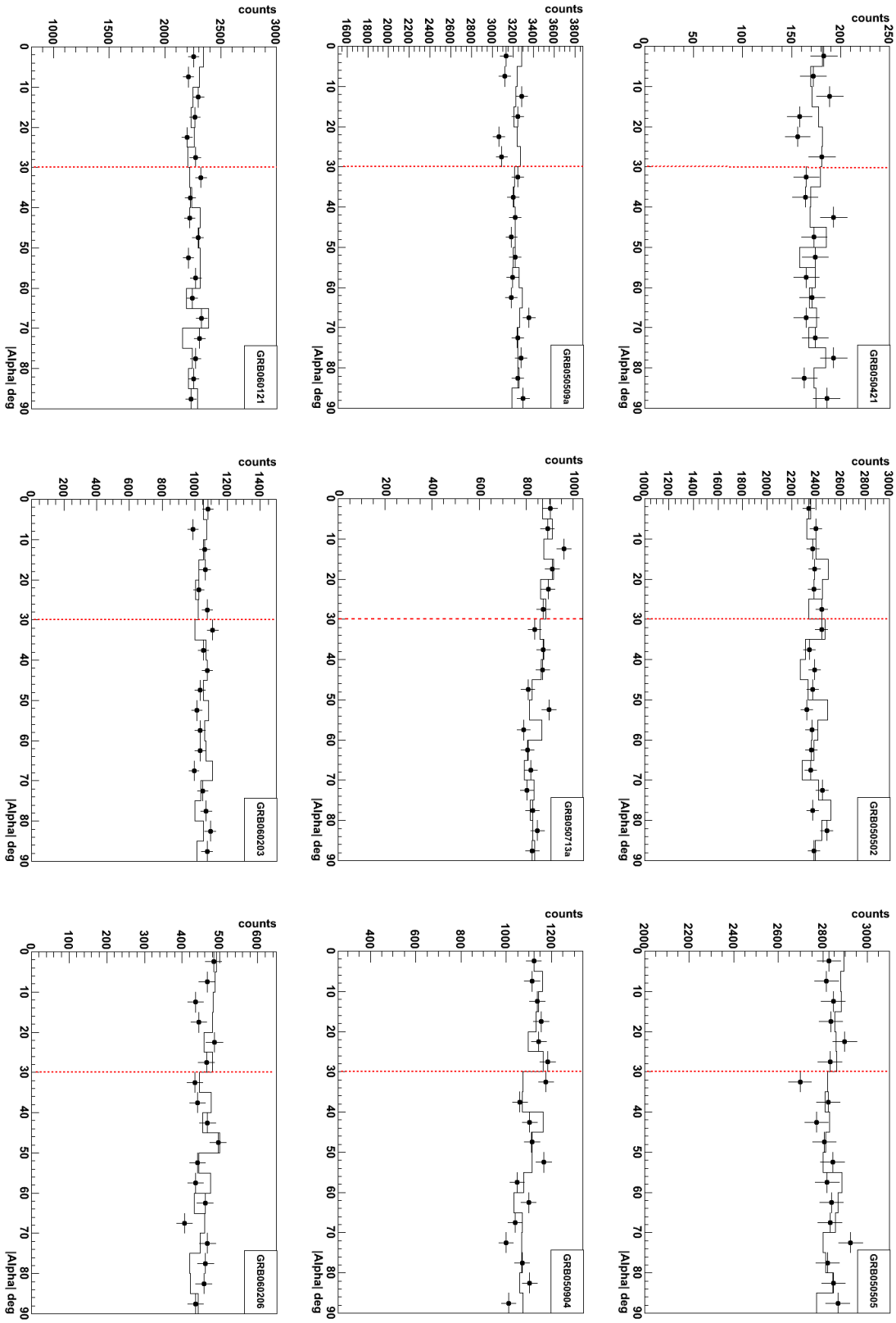

Fig. 10.— Alpha plots of all nine GRBs for the complete data set of each burst. Points with error bars refer to the burst data, the line refers to the background.

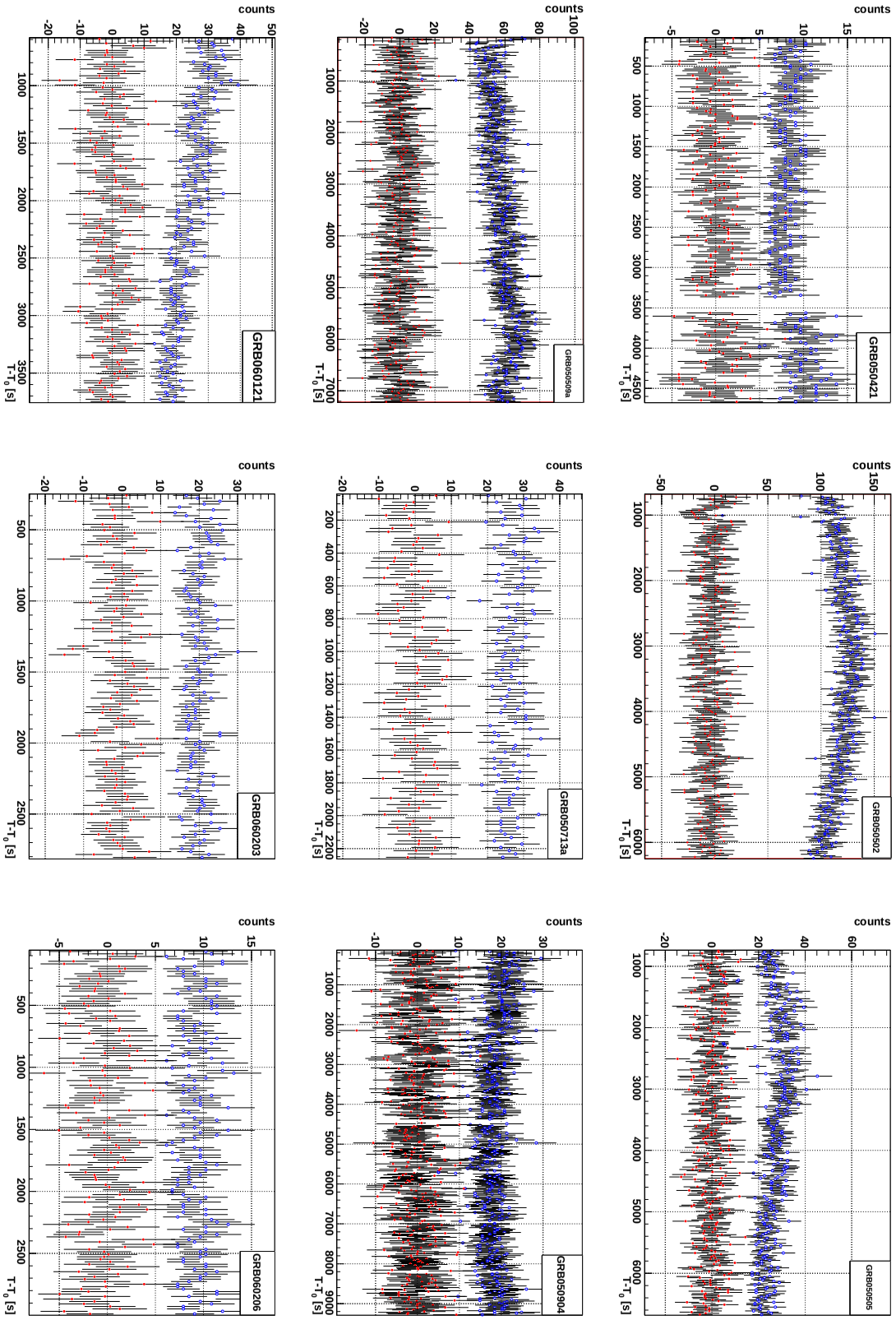

Fig. 11.— Light curves of all nine GRBs for the complete data set of each burst. The background rate of GRB 050502 is particularly high because of a higher night sky background due to the Moon light.

Arimoto, M., et al. 2006, GCN 4550

Atkins, R., et al. 2000, ApJ, 533, L119

Atkins, R., et al. 2005, ApJ, 630, 996

Bahcall, J. N., & Mészáros, P. 2000, Phys.Rev.Lett., 85, 1362

Barbier, L. M., et al. 2005a, GCN 3296

Barbier, L., et al. 2005b, GCN 3407

Barthelmy, S., et al. 2006, GCN 4656

Bastieri, D., et al. 2005, Proceedings of the 29$^{\rm th}$ ICRC, Vol. 4, 435, Pune (India)

Beloborodov, A. 2005, ApJ, 618, L13

Breiman, L. 2001, Machine Learning, 45, 5

Bretz, T., Dorner, D., & Wagner, R. (MAGIC Coll.) 2003, in Procs. 28$^{\rm th}$ ICRC, 2943, Tsukuba (Japan)

Bretz, T. (MAGIC Coll.) 2005, in Procs. 29$^{\rm th}$ ICRC, Vol. 4, 315, Pune (India)

Böttcher, M., & Dermer, C. D. 1998, ApJ 499 L131

Burrows, D., et al. 2005, Science 309, 1833

Chiang, J., Dermer, C. D. 1999, ApJ 512, 699

Connaughton, V., et al. 1997, ApJ, 479, 859

Cortina, J., et al. (MAGIC Collab.) 2005, Proc. of the 29$^{\rm th}$ ICRC, Vol. 5, 359, Pune (India)

Cummings, J., et al. 2005, GCN 3910

de Jager, O. C., & Stecker, F. W. 2002, ApJ, 566, 738

Derishev, E. V., Kocharovsky, V. V., & Khocarovsky, Vl. V. 1999, ApJ, 521, 640

Derishev, E. V., Kocharovsky, V. V., & Khocarovsky, Vl. V. 2001, A&A, 372, 1071

Dermer, C. D., Chiang, J., & Mitman, K. 2000, ApJ, 537, 785

Dingus, B. L. 1995, Ap&SS, 231, 187

Donaghy, T. Q., et al. 2006, astro-ph/0605570, proceeding at ApJ

Durig, D. T., 2005, IAUC 8521

Falcone, A., et al. 2005, GCN 3581

Fegan, D. J. 1997, J. Phys. G, 23, 1013

Fragile, P., et al. 2004, Astrop. Phys. 20, 598

Galante, N., et al. 2005, GCN 3747

Galante, N. 2006, Università degli Studi di Siena, Ph.D. Thesis (available at http://wwwmagic.mppmu.mpg.de/publications/theses/NGalante.pdf.gz)

Gaug, M., Bartko, H., Cortina, J., Rico, J. (MAGIC Coll.) 2005, in Procs. 29$^{\rm th}$ ICRC, Pune (India)

Gaug, M. 2006, Universitat Autònoma de Barcelona, Ph. D. Thesis (available at: http://magic.mppmu.mpg.de/publications/theses/MGaug.pdf)

Götting, N., et al. 2003, GCN 1007

Golenetskii, S., et al. 2005, GCN 3619

Golenetskii, S., et al. 2006, GCN 4564

González, M. M., Dingus, B. L., Kaneko, Y., Preece, R. D., Dermer, C. D., & Briggs, M. S. 2003, Nature, 424, 749

Gotz, D., et al. 2005a, GCN 3323

Gotz, D., et al. 2005b, GCN 3329

Guetta, D., Piran, T., Waxman, E. 2003, astroph/0311488

Hengstebeck, T. 2006, Humboldt-Universität zu Berlin, Ph. D. Thesis

Hillas, A. M. 1985, in Proc. 19$^{\rm th}$ ICRC, La Jolla, USA, Vol. 3, 445

Hullinger, D., et al. 2005 GCN 3364

Hurkett, C., et al. 2005a, GCN 3360

Hurkett, C., et al. 2005b, GCN 3379

Hurley, K., et al. 1994, Nature, 372, 652

Jarvis, B. (STACEE Coll.) 2005, in Procs. 29th ICRC, Vol. 4, 455, Pune (India)

Kawai, N., et al. 2005, GCN 3937

Levan, A. J., et al. 2006, GCN 4841

Li, Z., Dai, G., Lu, T. 2002, A&A 396, 303

Malesani, D., et al. 2006, GCN 4561

Mangano, V., et al. 2006, GCN 4565

Mannheim, K., Hartmann, D., Burkhardt, F. 1996, ApJ, 467, 532

Mereghetti, S., & Mowlavi, N. 2005, GCN 4084

Mészáros, P., Rees, M., Papathanassoiu, H. 1994, ApJ, 432 181

Mészáros, P. 2006, Rept.Prog.Phys. 69, 2259-2322

Mirzoyan, R. (MAGIC Coll.) 2005, in Procs. 29th ICRC, Vol. 4, 23, Pune (India)

Morris, D., et al. 2006a, GCN 4682

Morris, D., et al. 2006b, astro-ph/0602490, accepted by ApJ

Nikishov, A. I. 1961, Zh. Eksp. Teor. Fiz., 41, 549 (English transl. in Soviet Phys.-JETP Lett., 14, 392 [1962])

Padilla et al. 1998, A&A, 337, 43

Palmer, D., et al. 2005, GCN 3597

Palmer, D., et al. 2006, GCN 4697

Papathanassiou, H., & Mészáros, P. 2004, ApJ 471, L91

Pe'er, A., & Waxman, E. 2004, ApJ, 603, 448

Pilla, R.P., & Loeb, A. 1998, ApJ, 494, L167

Piran, T. 1999, Phys.Rep. 314, 575

Poirer, J., et al. 2003, Phys.Rev.D67:042001

Preece, R. D., Briggs, M. S., Mallozzi, R. S., Pendleton, G. N., Paciesas, W. S, & Band, D. L. 2000, ApJS, 126, 19

Razzaque, S., Mészáros, P., Zhang, B. 2004, ApJ, 613, 1072

Rolke, W., López, A., & Conrad, J. 2005, Nucl. Instr. & Meth. A, 551, 493

Rossi, E., Beloborodov, A., & Rees, M.J. 2006, MNRAS 369, 1797

Sakamoto, T., et al. 2005, GCN 3938

Saz Parkinson, P., et al. 2005a, GCN 3411

Saz Parkinson, P., et al. 2005b, GCN 4249

Saz Parkinson, P., et al. 2005c, GCN 4265

Saz Parkinson, P., et al. 2006a, GCN 5061

Saz Parkinson, P., et al. 2006b, GCN 5527

Scapin, V., et al. 2006, in Proc. Swift and GRBs, Unveiling the Relativistic Universe, Venice (Italy)

Totani, T. 2000, ApJ, 536, L23

Wang, X., Dai, Z., & Li, Z. 2001, ApJ, 556, 1010

Wang, X., Li, Z., & Mészáros, P. 2006, ApJ, 641, L89

Waxman, E. 1995, Phys. Rev. Lett. 75, 386

Yost, S.A., et al. 2006, ApJ, 636, 959-966

Zhang, B., & Mészáros, P. 2001, ApJ, 559, 110

Zhou, X., et al. 2003, in Procs. 28$^{\rm th}$ ICRC, 2757, Tsukuba (Japan)